# Parameterization of the Inverse Error Covariances for SWOT Altimetry

**Max Yaremchuk[1], Joseph M. D'Addezio[2], Gleb Panteleev[1], and Gregg A. Jacobs[1]**

[1]Naval Research Laboratory, Ocean Dynamics and Prediction, Mississippi USA

[2]University of Southern Mississippi, School of Ocean Sciences and Technology, Division of Marine Science, Mississippi USA

## 0. Introduction

High-resolution (swath) altimeter missions scheduled to monitor the ocean surface in the near future have observation error covariances (OECs) with slowly decaying off-diagonal elements. This property presents a challenge for the majority of the data assimilation (DA) algorithms which were designed under the assumption of the diagonal OECs being easily inverted. We present a method of approximating the inverse of a dense OEC by a sparse matrix represented by the polynomial of spatially inhomogeneous differential operators, whose coefficients are optimized to fit the target OEC by minimizing a quadratic cost function. Explicit expressions for the cost function gradient and the Hessian are derived. The method is tested with an OEC model generated by the SWOT simulator.

## 1. Approximating the inverse covariance

Consider an approximation $\mathbf{R}_m$ to the sample SSH covariance **R** of the form

$$\mathbf{R}_m = \mathbf{A} + \nabla^{\mathsf{T}}\mathbf{B}\nabla + \Delta\mathbf{C}\Delta \qquad (1)$$

where $\nabla$ is the $2N\text{-}n_x\text{-}n_y \times N$ matrix ($N=n_xn_y$), representing the first-order approximation of the gradient operator on a 2d grid, $\Delta = \nabla^{\mathsf{T}}\nabla$ is the Laplacian, and **A**, **B**, **C** are sparse control matrices. Their $M = 4N\text{-}n_x\text{-}n_y$ non-zero elements populating the $M$-dimensional vector **x** are optimized by minimization of the quadratic cost function, measuring the Frobenius norm $\|\,.\,\|_F$ of the respective residual:

$$J = \|\mathbf{R}_m\mathbf{R} - \mathbf{I}\|_F^2 \qquad (2)$$

where **I** is the identity matrix. The gradient of $J$ is linear in **x** and has the form

$$\frac{\delta J}{\delta \mathbf{A}} = \mathbf{Q}; \qquad \frac{\delta J}{\delta \mathbf{B}} = \nabla\mathbf{Q}\nabla^{\mathsf{T}}; \qquad \frac{\delta J}{\delta \mathbf{C}} = \Delta\mathbf{Q}\Delta$$

Where $\mathbf{Q}=2(\mathbf{R}_m\mathbf{R}^2 - \mathbf{R})$. The system of equations for finding the optimal value of **x** can be written in the form **Hx** = **r** with the following Hessian matrix **H** and the right-hand side **r**:

$$\mathbf{H} = \begin{bmatrix} \mathbf{R}^2 \circ \mathbf{I} & \mathbf{R}^2\nabla^{\mathsf{T}} \circ \nabla^{\mathsf{T}} & \mathbf{R}^2\Delta \circ \Delta \\ \nabla\mathbf{R}^2 \circ \nabla & \nabla\mathbf{R}^2\nabla^{\mathsf{T}} \circ \nabla\nabla^{\mathsf{T}} & \nabla\mathbf{R}^2\Delta \circ \nabla\Delta \\ \Delta\mathbf{R}^2 \circ \Delta & \Delta\mathbf{R}^2\nabla^{\mathsf{T}} \circ \Delta\nabla^{\mathsf{T}} & \Delta\mathbf{R}^2\Delta \circ \Delta^2 \end{bmatrix}. \quad \mathbf{r} = \begin{bmatrix} \mathbf{R} \\ \nabla\mathbf{R}\nabla^{\mathsf{T}} \\ \Delta\mathbf{R}\Delta \end{bmatrix}$$

Where $\circ$ denotes Hadamard element-wise matrix product. The latter relationships could be useful for constructing block-diagonal preconditioners for the iterative solvers of the system **Hx**=**r**, or for its direct solution on the moderate-size ($N < 10^4$) grids.

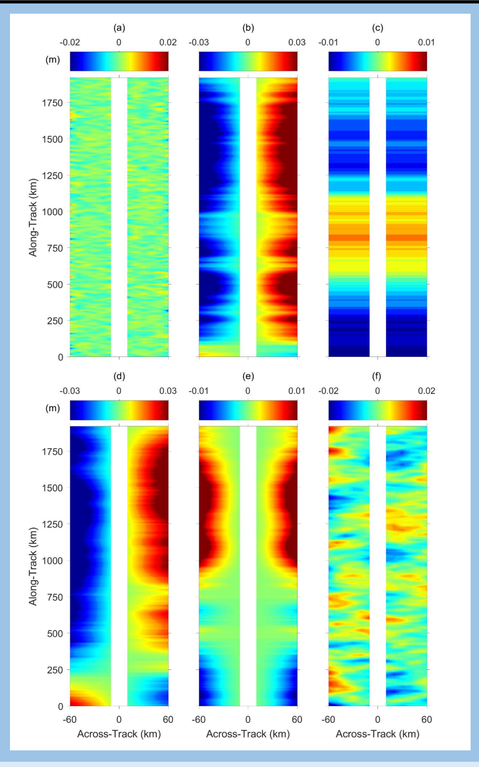


Figure 1. Random iteration of SWOT simulator derived along- and across-track errors. The individual error fields are: (a) Karin noise, (b) roll error, (c) timing error, (d) phase error, (e) baseline error, and (f) wet troposphere error.

## 2. Numerical Testing

The ansatz (1) for the approximation of the inverse observation error covariance was tested with the target OEC generated by the Jet Propulsion Laboratory's (JPL) SWOT simulator (**Ubelmann et al, 2017**). The simulator generates realizations of SSH observation error fields based on the latest estimate of the SWOT error budget. The error field contains six constituents: Ka-band radar interferometer noise, wet tropospheric error, and errors associated with uncertainties in the estimation of roll, phase, baseline, and timing of the SWOT observational platform (**Figure 1)**. With a reasonable degree of accuracy, the first two error fields can be considered to be uncorrelated. The remaining four error sources are of particular interest because they are highly correlated over large spatial scales. As shown by **Ruggiero et al (2016),** these errors are characterized by typical decorrelation scales of several hundred kilometers along the swath and approximately a hundred across, with the marginal pointwise pdfs being very close to Gaussian.

In generating the target OEC matrix, we used the SWOT simulator version 2.0.0 with the following parameters: the default cut off wavelength of 40,000 km and a 2 beam wet tropospheric error correction. Additionally, anticipating large decorrelation scales and the absence of smaller-scale spatial variability in the matrix columns, we elected 40 and 10 km sampling in the along- and across-track directions respectively. This selection also decreased the influence of uncorrelated Ka-band noise on the OEC structure. 5,000 random realizations of all error sources summed together were generated by having the simulator recursively sample the same 21 day repeat orbit over a subdomain of the Western Pacific (116ºE-133ºE, 18ºN-34ºN) with a total sampled track length of 2000 km and width of 140 km. Excluding the grid points in the 20 km wide nadir gap, the sampled OEC field dimensions were $n_x$=14, $n_y$ =51, ($N=n_xn_y$ =714) with the total number of adjusted degrees of freedom $M$ = 2,791 and the number of the independent elements in the target covariance matrix $N(N+1)/2$=255,255.The resulting error fields were characterized by approximately Gaussian pointwise pdfs with the average magnitude of the means ~$10^{-4}$ m and the standard deviations varying between of 0.03 m near the nadir gap and 0.31 m at the swath periphery.

## 3. Comparison with 5-parameter model

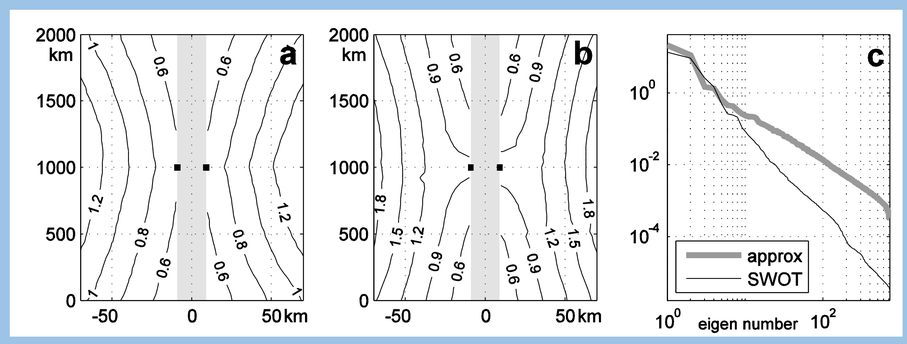


Figure 2. (a) Map of the sum of two columns of the SWOT covariance matrix **R** (column positions shown by squares) and (b) its approximation by $\mathbf{R}_m^{-1}$. (c) the spectra of the SWOT covariance (thin black line) and its approximation. Covariance values are divided by 100 cm$^2$.

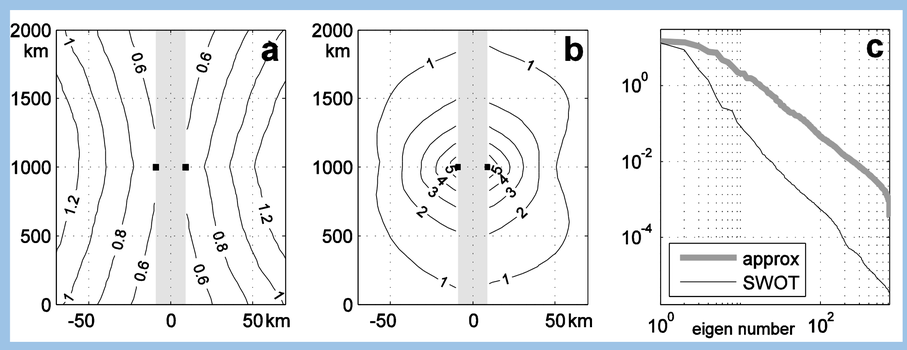


Figure 3. Same as Figure 2, but the inverse covariance model is described by Ruggiero et al. (2016).

**Figure 2** shows half the sum of the OEC fields corresponding to the pair of SSH observations located on both edges of the nadir gap in the center of the sampled track. Similar to the results of **Ruggiero et al (2016),** covariance structures at intermediate scales are barely visible. However, there is a strong anisotropy of the covariance with the typical OEC spatial scales in the along- and across-track directions differing by an order in magnitude (600 km and 60 km respectively).

**Figure 2a** and b demonstrate the result of approximating **R** by the inverse covariance model (1). Due to the limited number of ensemble members a slight asymmetry (of the order of 1%) has been observed in the structure of the mirror rows of **R**. Figure 2b shows that this asymmetry is considerably enhanced in the approximating matrix $\mathbf{R}_m^{-1}$ (cf. **Fig. 2a**, **b**). The effect is caused by the coarse resolution of the nadir gap which is only 2 grid steps wide, and associated errors in the finite-difference approximation of $\mathbf{R}_m^{-1}$ by the ansatz (1).

Due to the modest dimension of the control space ($M$ = 2,791) and low condition number (cond(**H**)=2 $10^4$) of the Hessian matrix, the optimization took a few seconds on a single CPU of a PC using the MatLab sparse system solver. As it is seen, the algorithm provides a reasonably accurate fit to the leading eigenmodes of **R** (**Figure 2c**) with the relative error Tr( $\mathbf{R}_m^{-1}$- **R**)/Tr(**R**) of 22%.

As a matter of comparison, we performed approximation of $\mathbf{R}^{-1}$ in the reduced 5-dimensional space proposed by **Ruggiero et al (2016)**, who assigned a fixed spatial variability to the diagonals of the control matrices and minimized the cost function (2) by varying five diagonal scaling factors. In this procedure, we employed the technique of Section 1, which can be viewed as a generalization of the computational approach of **Ruggiero et al (2016)**, who used five-fold expansion of the data space by computing the derivatives of the error fields in SWOT simulator output instead of explicit computation of the Hessian and its projection on the reduced control space.

**Figure 3** shows the results of the reduced space optimization. As it is seen, the reduced method provides a poorer fit to the SWOT spectrum being tested (cf. **Fig. 2c** and **3c**) and a larger error in approximating the columns of the SWOT covariance matrix (cf. **Fig. 2b,3b** and **Fig. 2a**). This should be attributed to lesser flexibility of the reduced procedure, as the number of adjusted parameters is approximately 2,791/5~560 times smaller compared to the case of full optimization involving solution of the equation **Hx**=**r**.

## 4. Summary and Conclusions

1. A methodology of approximating the inverse OECs by sparse matrices with a predefined sparsity pattern is proposed.
2. The sparsity pattern is defined by the 2nd-order polynomial in differential operators acting on diagonal control matrices whose non-zero elements are adjusted to minimize the Frobenius norm of the approximation error.
3. Explicit relationships for the cost function gradient and the Hessian matrix of the optimization problem have been obtained.

## Acknowledgments

This research is funded the Naval Research Laboratory base program Submesoscale Prediction of Eddies by Altimeter Retrieval (SPEAR). Joseph M. D'Addezio is supported by the Naval Research Laboratory Cooperative Agreement BAA-N00173-03-73-13-01 awarded to The University of Southern Mississippi.

## References

1. Yaremchuk et al, 2018. *Quarterly J. Royal Metorol. Soc.*, **141** (in press).
2. Ruggiero et al, 2016. *J. Ocean and Atm. Tech.*, **141**, 2755-2768.
3. Ubelmann et al,, 2017. SWOT simulator for ocean science. Documentation, release 2.3.0 [Available online at *https://swot.oceansciences.org/docs/documentation swotsimulator.pdf*].